Supporting Information

Synergistic effect of defect passivation and energy level adjustment for low-temperature carbon-based $CsPbI_2Br$ perovskite solar cells

*Xiang Zhang[a], Dan Zhang[a], Tonghui Guo[b], Chunqiu Zhengc[c], Yuan Zhou[a], Junjun Jin[a], Zhenkun Zhu[a], Zhen Wang[a], Xiaxia Cui[a], Sujuan Wu[c], Jing Zhang[b], Qidong Tai[a]**

[a] The Institute of Technological Sciences, Wuhan University, Wuhan 430072, P. R. China.

[b] Department of Microelectronic Science and Engineering, Ningbo University, Zhejiang 315211, P. R. China.

[c] Institute for Advanced Materials, South China Academy of Advanced Optoelectronics, South China Normal University, Guangzhou 510006, P. R. China.

*Corresponding Authors: qdtai@whu.edu.cn

Experimental Section

Material

Indium-doped tin oxide (ITO, sheet resistance: 7-9 Ω sq^{-1}) glass, lead (II) bromide ($PbBr_2$, 99.999%), phenylethylammonium iodide (PEAI, 99.9%), phenylethylammonium bromide (PEABr, 99.9%) and cesium iodide (CsI, 99.999%) were bought from Advanced Election Technology Co., Ltd. Tin (IV) oxide (SnO_2) colloid precursor (15 wt% in H_2O colloidal dispersion) was obtained from Alfa Aesar. Lead(II) iodide (PbI_2, 99.99%), 4-fluorophenylethylammonium iodide (P-F-PEAI), 4-fluorophenylethylammonium bromide (P-F-PEABr) and poly (3, 4-ethylenedioxythiophene):poly (styrenesulfonate) (PEDOT:PSS) were purchased from Xi'an Polymer Light Technology Corp. Lead(II) acetate trihydrate ($Pb(Ac)_2$, 99.999%), N,N-Dimethylformamide (DMF, 99.8%), Dimethyl sulfoxide (DMSO, ≥ 99.9%) and ethyl acetate (EA, 99.8%) were provided by Sigma-Aldrich. Isopropyl alcohol (IPA, ≥ 99.9%), zinc acetate dihydrate ($Zn(Ac)_2 \cdot 2H_2O$, 99.995%), ethanolamine (standard for GC, >99.5%), and 2-Methoxyethanol (anhydrous, 99.8%) were obtained from Aladdin. Conductive carbon pastes were bought from Jujo Printing Supplies & Technology (Pinghu) Co., Ltd. Absolute ethanol and acetone were gotten from Sinopharm. PbI_2(DMSO) and $PbBr_2$(DMSO) adducts were synthesized according to the previous works.[1, 2]

Device fabrication

Etched ITO glass substrate (1.5 cm × 1.5 cm) was sequentially cleaned with detergent, deionized water, acetone, IPA, and absolute ethanol under sonication for 20 min, respectively. Later, it was dried by the nitrogen (N_2) flow and was treated with ultraviolet (UV)-ozone for 5 min. The SnO_2 ETL was deposited on the ITO glass substrate by spin-coating diluted SnO_2 solution (2.67 wt% in deionized water) at 500 rpm for 3 s and 4000 rpm for 30 s, followed by annealing at 150 °C for 30 min in ambient air. It was treated with UV-ozone for 10 min, the pre-prepared ZnO solution (250 mg $Zn(Ac)_2 \cdot 2H_2O$ was dissolved in 10 ml 2-Methoxyethanol and 275 ul ethanolamine and stirred for 12 h) was spin-coated on the SnO_2 ETL at 500 rpm for 3 s and 4000 rpm for 60 s and annealed at 150 °C for 30 min in ambient air. After naturally cooling down, the glass/ITO/SnO_2/ZnO substrate was moved into a N_2-filled glovebox for perovskite and carbon electrode deposition. To obtain the $CsPbI_2Br$ precursor solution, 234 mg CsI, 243 mg PbI_2(DMSO), 200 mg $PbBr_2$(DMSO) and 5 mg $Pb(Ac)_2$ were added in 1 mL mixed solvents of DMSO and DMF (1:4, *v/v*) and stirred at 70 °C for 12 h. The prepared precursor solution was filtered with PTFE filter (0.22 μm), and then was spin-coated onto the glass/ITO/SnO_2/ZnO substrate at 1000 rpm for 10 s and 4000 rpm for 40 s. In the last 20 s of second step, 150 μL anti-solvent EA was quickly dropped onto the precursor film. The obtained precursor film was annealed at 120 ^{o}C for 10 min. For the passivation layers, the IPA precursor solution with various concentrations of PEAI, PEABr, P-F-PEAI or P-F-PEABr was dropped onto the $CsPbI_2Br$ surface and allowed to stand for 2 min before spin-coating. After that, they were spin-coated on the $CsPbI_2Br$ films at 3000 rpm for 30 s and baked at 100 °C for 15 min. Finally, conductive carbon paste was deposited on the sample surface by the doctor-blade technique and annealed at 120 °C for 20 min to evaporate the residual solvents. The device active area is 0.09 cm^2.

Characterization

The current density-voltage (*J-V*) characteristics were recorded by an Oriel So1 3A solar simulator (Newport, USA) with a Keithley 2400 source meter under a simulated AM 1.5G solar illumination. The light intensity (P_{light}) was calibrated to be 100 mW cm^{-2} by a National Renewable Energy Laboratory (NREL)-certified standard silicon solar cell. The reverse voltage scan rate (from 1.5 to 0 V) was 100 m V s^{-1} with a delay time of 50 ms. The external quantum efficiency (EQE) spectra were collected with a standard EQE system (Newport 66902, USA). The crystal structure was obtained by an X-ray diffractometer (XRD, Bruker D8 Advance, Germany) with Cu $K\alpha$ (λ = 1.5406 Å) radiation source at 40 kV and 40 mA. The chemical binding energy was monitored by an X-ray photoelectron spectrometer (XPS, Thermo Scientific K-Alpha+, USA) with an Al $K\alpha$ (hv = 1486.6 eV) radiation source. Fourier-transform infrared spectroscopy (FTIR) spectra were collected using a Nicolet iS5 instrument (Thermo Scientific, USA) with an iD7 ATR-diamond. The morphologies and energy-dispersive X-ray (EDX) elemental mapping were tested using a field-emission scanning electron microscopy (SEM, Zeiss SIGMA, Germany). The root mean square (RMS) roughness was investigated by the Nano Wizard 4 atomic force microscopy (AFM, JPK Inc. Germany). The UV-visible (UV-vis) absorption spectra were recorded on the UV-vis near-infrared spectrophotometer (Shimadzu UV-2600i, Japan). Steady-state photoluminescence (PL) and time-resolved PL (TRPL) decay spectra were performed with a fluorescence spectrometer (HORIBA DeltaFlex, U.K.) with excitation wavelength of 485 nm. The ultraviolet photoelectron spectroscopy (UPS) was measured using an ESCALAB Xi+ system (Thermo Fisher, USA). The electrochemical impedance spectroscopy (EIS), transient photovoltage (TPV), transient photocurrent (TPC), and capacitance-voltage (C^{-2}-V) measurements were conducted on an electrochemical workstation (Zahner, Germany). The dark J-V curves were detected by a Keithley 2400 source meter with a scan rate of 100 mV s^{-1}. The contact angles were measured using an optical goniometer (Dataphysics OCA 20, Germany) by drop casting a single drop (0.01 mL) of H_2O on the perovskite film and analyzed with its software. The photograph was taken after the H_2O droplet was in contact with the perovskite film for 1 s. Unless otherwise specified, all measurements were carried out in ambient air (25 °C, 20-30% relative humidity (RH)).

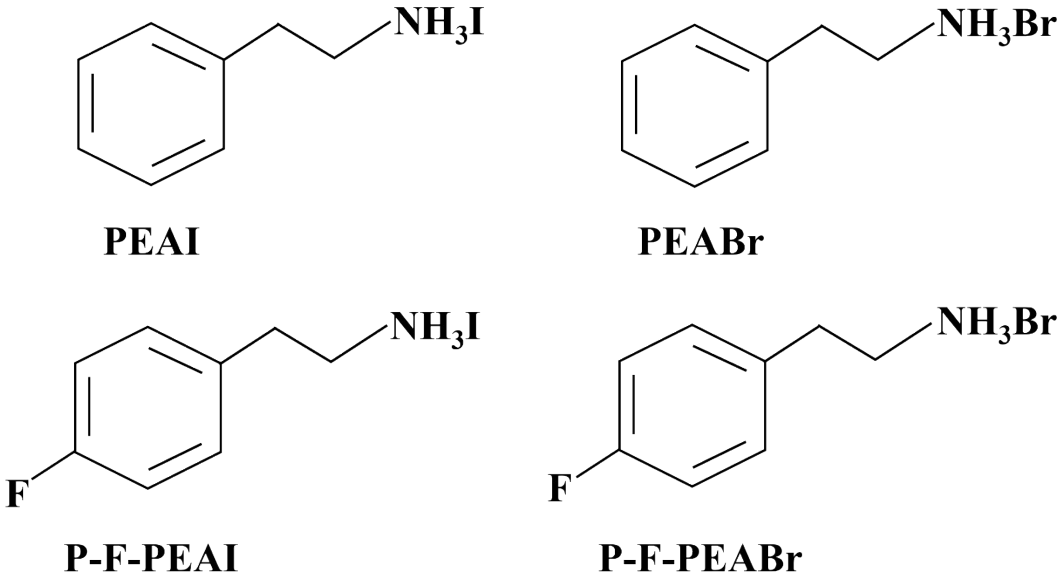

Fig. S1 Molecular structures of PEAI, PEABr, P-F-PEAI and P-F-PEABr.

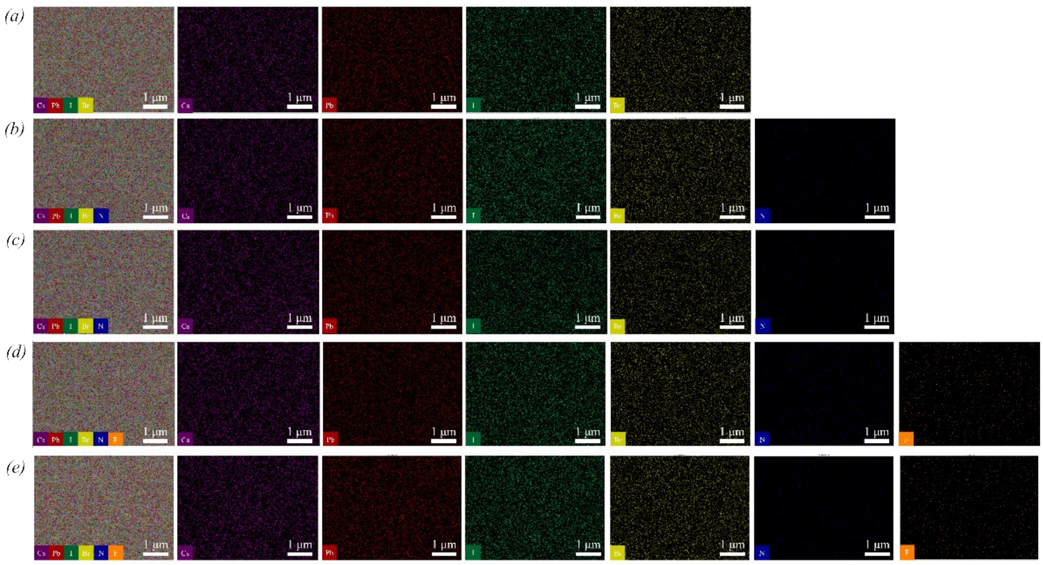

Fig. S2 EDX elemental mapping of reference and passivated $CsPbI_2Br$ films: (a) reference, (b) PEAI, (c) PEABr, (d) P-F-PEAI and (e) P-F-PEABr.

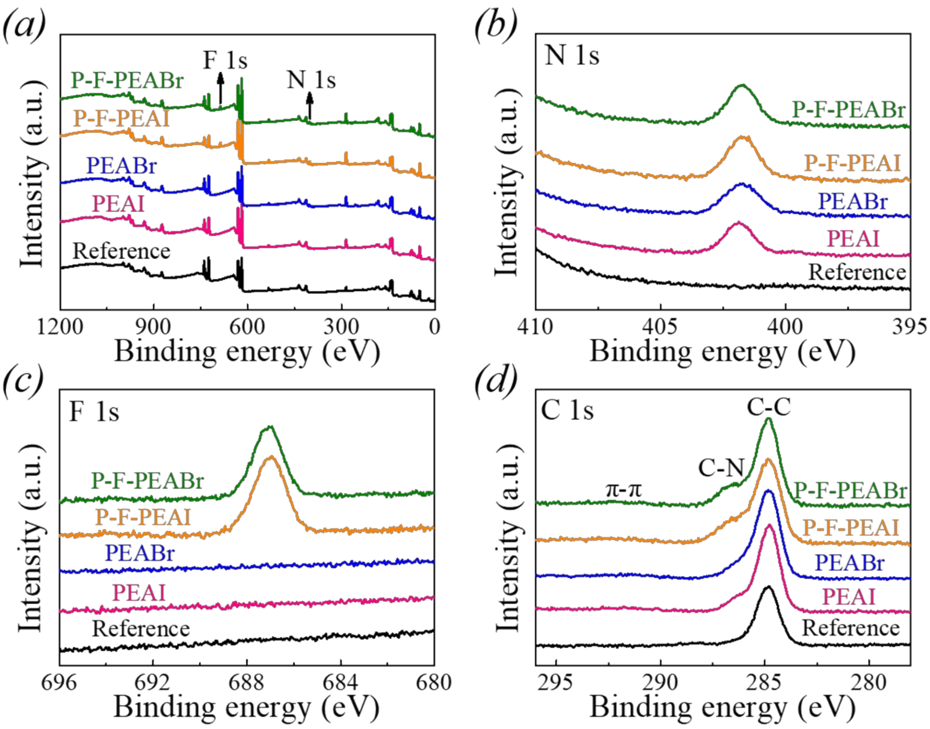

Fig. S3 (a) Full XPS survey spectra, (b) N 1s, (c) F 1s and (d) C 1s XPS spectra of reference and passivated $CsPbI_2Br$ films.

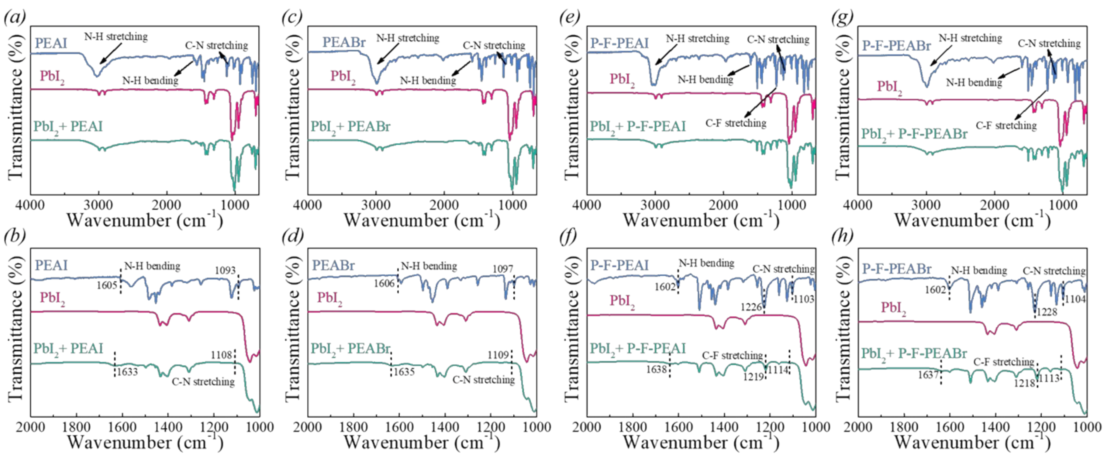

Fig. S4 FTIR spectra of organic ammonium halide salts powders, PbI_2 powders, and organic ammonium halide salts/PbI_2 mixed powders. Mixed powders were obtained by dissolving them in 1 ml DMSO at 70 °C under stirring for 12 h, followed by the removal of DMSO solvent by rotary evaporation and drying in a vacuum oven at 60 °C for 48 h. The molar mass of PbI_2 is 0.9 M. The mass ratio of organic ammonium halide salts/PbI_2 is 1:5.

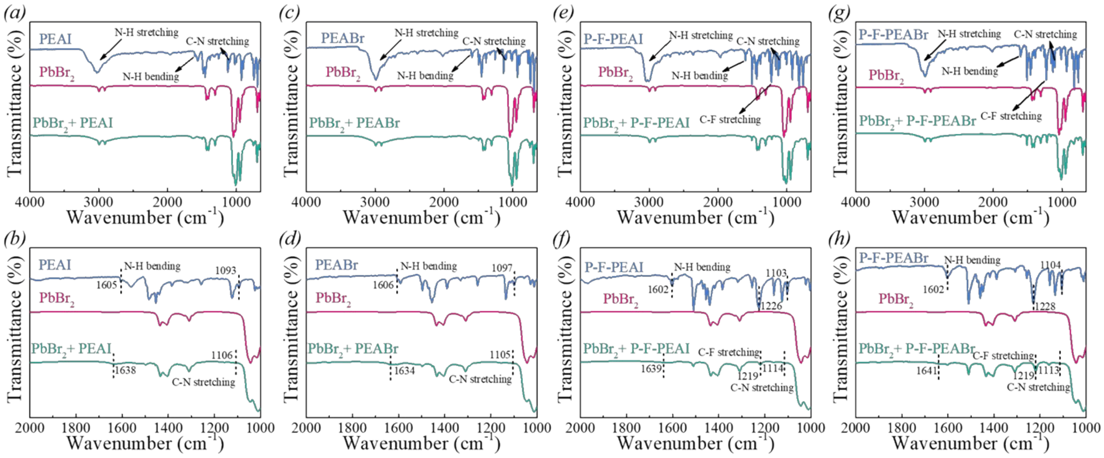

Fig. S5 FTIR spectra of organic ammonium halide salts powders, $PbBr_2$ powders, and organic ammonium halide salts/$PbBr_2$ mixed powders. Mixed powders were obtained by dissolving them in 1ml DMSO at 70 °C under stirring for 12 h, followed by the removal of DMSO solvent by rotary evaporation and drying in a vacuum oven at 60 °C for 48 h. The molar mass of $PbBr_2$ is 0.9 M. The mass ratio of organic ammonium halide salts/$PbBr_2$ is 1:5.

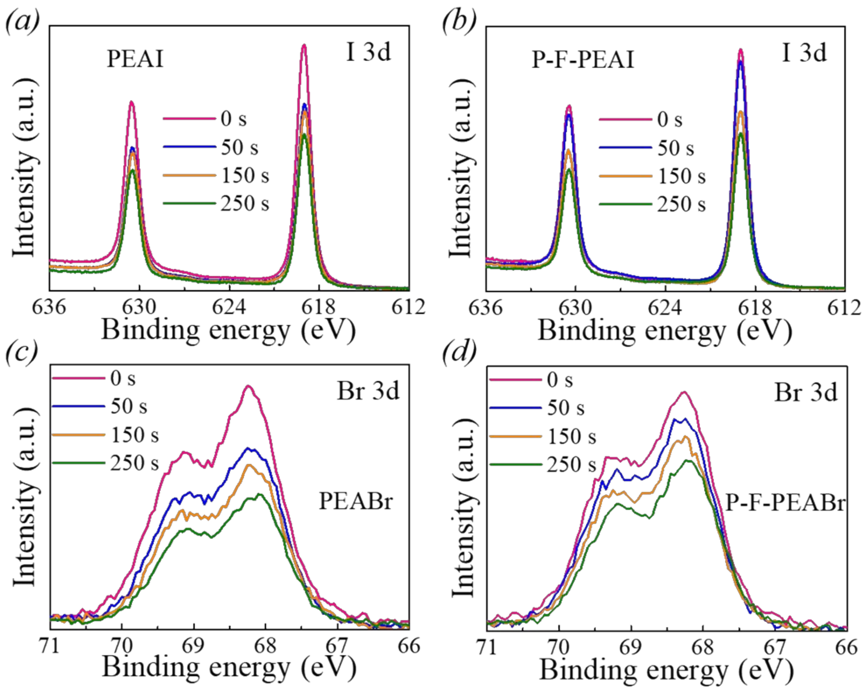

Fig. S6 XPS depth spectra of I 3d and Br 3d in the passivated $CsPbI_2Br$ films: (a) PEAI, (b) P-F-PEAI, (c) PEABr, (d) P-F-PEABr.

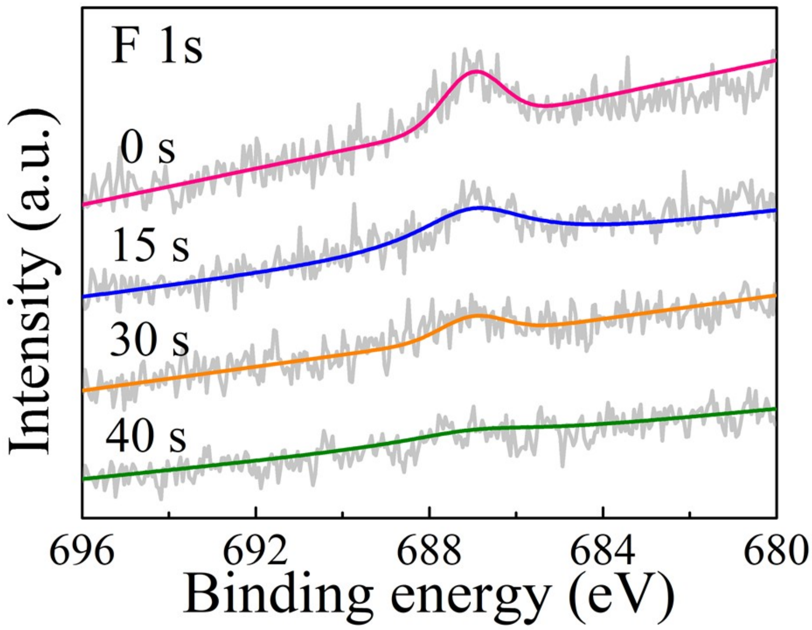

Fig. S7 XPS depth spectra of F 1s in the P-F-PEABr passivated $CsPbI_2Br$ films.

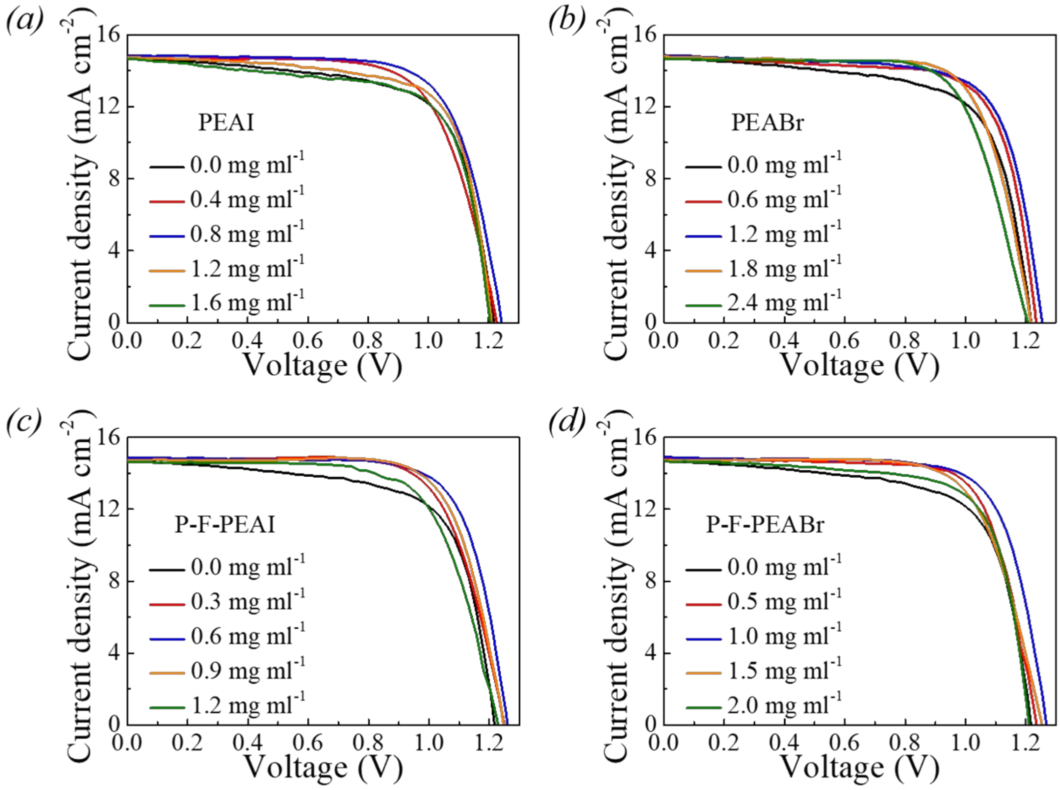

Fig. S8 *J-V* curves for $CsPbI_2Br$ C-IPSCs passivated by the organic ammonium halide salts with different precursor solution concentrations: (a) PEAI, (b) PEABr, (c) P-F-PEAI and (d) P-F-PEABr.

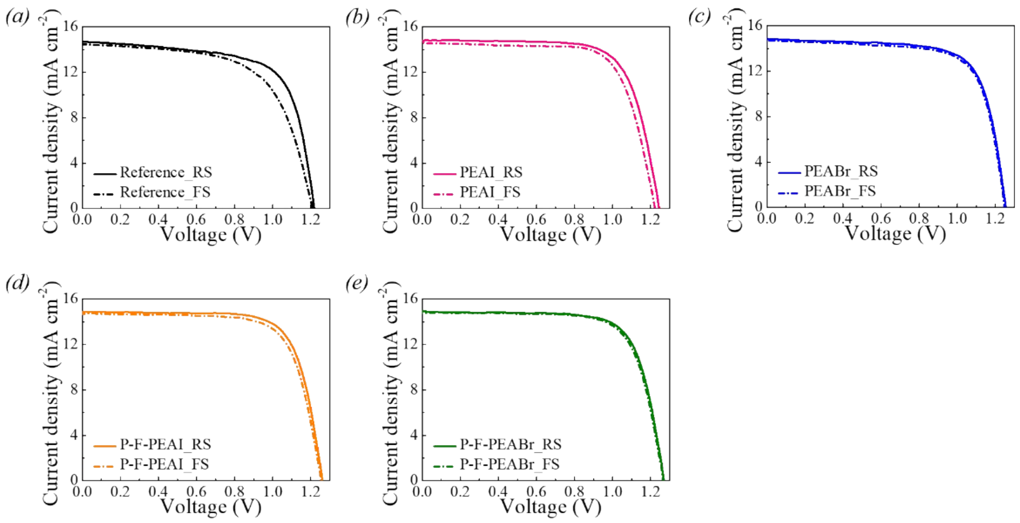

Fig. S9 *J-V* curves for various carbon-based $CsPbI_2Br$ PSCs under both the reverse scan (*RS*) and forward scan (*FS*) directions: (a) reference, (b) PEAI, (c) PEABr, (d) P-F-PEAI and (e) P-F-PEABr.

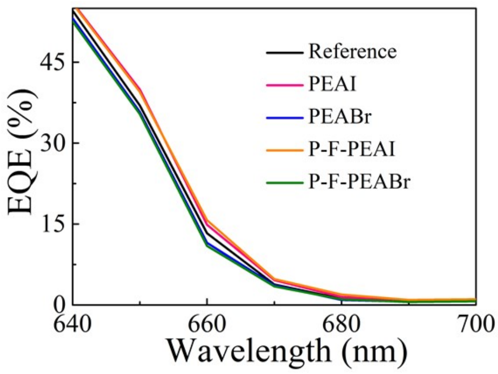

Fig. S10 Enlarged view of EQE curves at long wavelengths.

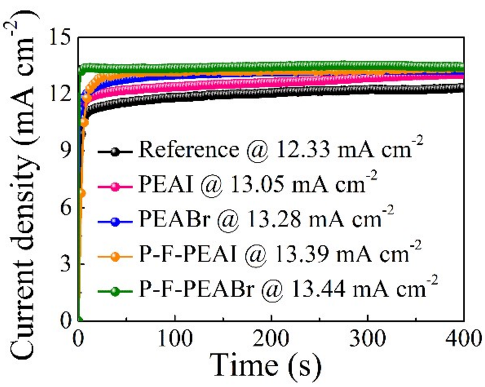

Fig. S11 SPO curves of J_{sc} for reference and passivated devices at their maximum power points.

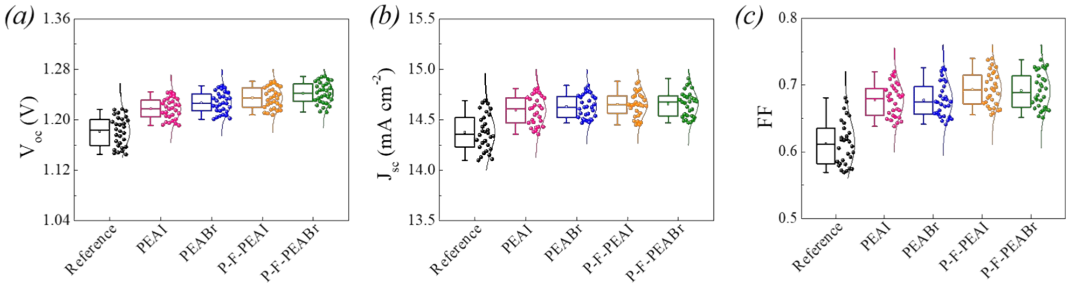

Fig. S12 (a) V_{oc}, (b) J_{sc} and (c) FF distributions of reference and passivated devices from 30 individual C-IPSCs.

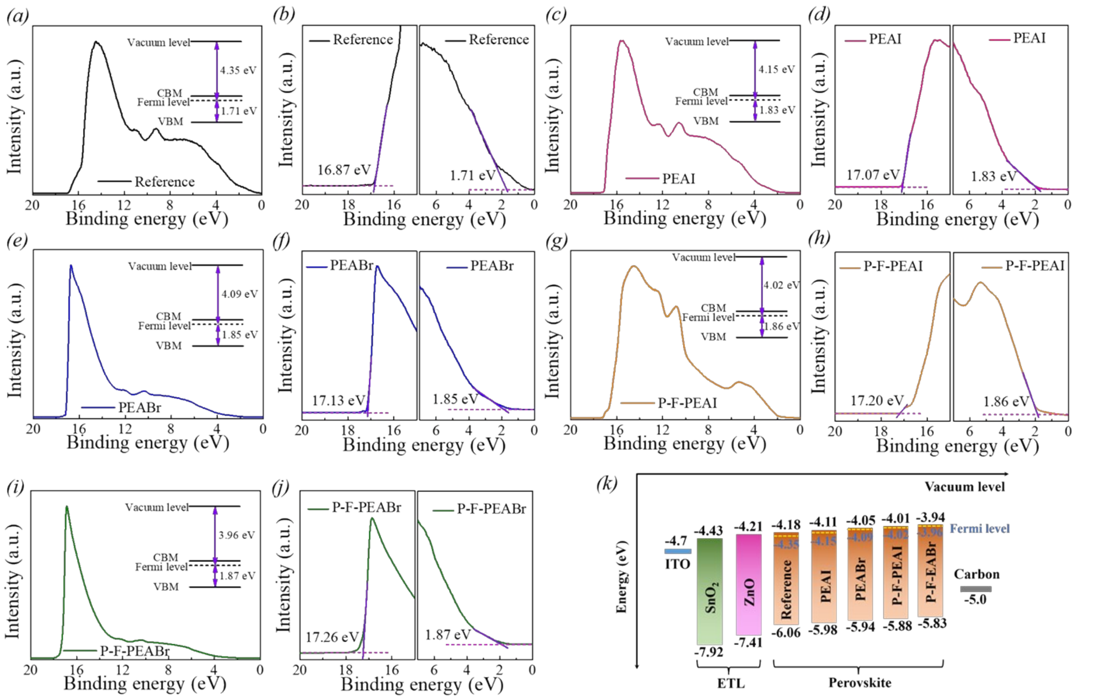

Fig. S13 UPS spectra of secondary electron cut-off ($E_{cut\text{-}off}$) and onset (E_{onset}) energy of reference and passivated $CsPbI_2Br$ films: (a-b) reference, (c-d) PEAI, (e-f) PEABr, (g-h) P-F-PEAI and (i-j) P-F-PEABr. (k) Energy level diagram of corresponding materials used in the $CsPbI_2Br$ C-IPSCs.

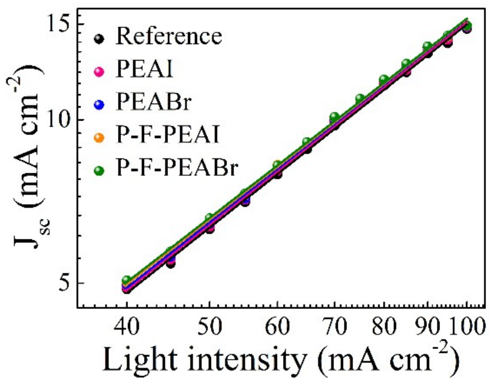

Fig. S14 J_{sc} versus P_{light} for reference and passivated devices.

Table S1. Fitting parameters of TRPL decay spectra of reference and passivated $CsPbI_2Br$ films on the glass substrate.

Sample	A_1	τ_1 (ns)	τ_1 (%)	A_2	τ_2 (ns)	τ_2 (%)	τ_{pl} (ns)
Reference	0.58	8.58	19.47	0.74	27.81	80.53	24.07
PEAI	0.56	33.37	69.75	0.78	10.39	30.25	26.42
PEABr	0.47	11.31	14.26	0.73	43.78	85.74	39.15
P-F-PEAI	0.38	13.17	8.21	0.76	73.60	91.79	68.64
P-F-PEABr	0.32	11.45	5.41	0.81	79.05	94.59	75.39

Table S2. The V_{TFL} and N_{trap} values of hole-only devices with the architecture of ITO/PEDOT:PSS/$CsPbI_2Br$/with or without the passivation layers/carbon.

Device	Reference	PEAI	PEABr	P-F-PEAI	P-F-PEABr
V_{TFL} (V)	1.82	1.65	1.34	1.25	1.19
N_{trap} (10^{16} cm^{-3})	1.50	1.36	1.10	1.03	0.98

Table S3. Photovoltaic parameters of $CsPbI_2Br$ C-IPSCs passivated by the PEAI with different precursor solution concentrations.

Concentration (mg ml^{-1})	V_{oc} (V)	J_{sc} (mA cm^{-2})	FF	PCE (%)
0.0	1.217	14.69	0.681	12.18
0.4	1.227	14.73	0.696	12.58
0.8	1.244	14.81	0.720	13.27
1.2	1.212	14.76	0.716	12.81
1.6	1.205	14.64	0.695	12.26

Table S4. Photovoltaic parameters of $CsPbI_2Br$ C-IPSCs passivated by the PEABr with different precursor solution concentrations.

Concentration (mg ml^{-1})	V_{oc} (V)	J_{sc} (mA cm^{-2})	FF	PCE (%)
0.0	1.217	14.69	0.681	12.18
0.6	1.234	14.70	0.730	13.24
1.2	1.254	14.84	0.726	13.51
1.8	1.216	14.75	0.733	13.15
2.4	1.204	14.66	0.711	12.55

Table S5. Photovoltaic parameters of $CsPbI_2Br$ C-IPSCs passivated by the P-F-PEAI with different precursor solution concentrations.

Concentration (mg ml^{-1})	V_{oc} (V)	J_{sc} (mA cm^{-2})	FF	PCE (%)
0.0	1.217	14.69	0.681	12.18
0.3	1.250	14.77	0.718	13.26
0.6	1.261	14.88	0.740	13.89
0.9	1.249	14.73	0.738	13.58
1.2	1.229	14.64	0.690	12.42

Table S6. Photovoltaic parameters of $CsPbI_2Br$ C-IPSCs passivated by the P-F-PEABr with different precursor solution concentrations.

Concentration (mg ml^{-1})	V_{oc} (V)	J_{sc} (mA cm^{-2})	FF	PCE (%)
0.0	1.217	14.69	0.681	12.18
0.5	1.235	14.80	0.739	13.51
1.0	1.269	14.91	0.738	13.97
1.5	1.253	14.72	0.710	13.10
2.0	1.211	14.65	0.718	12.74

Table S7. Performance comparisons of $CsPbI_2Br$ C-IPSCs reported to date.

No.	Device structure	$CsPbI_2Br$ annealing temperature (°C)	V_{oc} (V)	J_{sc} (mA cm^{-2})	FF	PCE (%)	Ref.
1	ITO/SnO_2/ZnO/$CsPbI_2Br$/P-F-PEABr/carbon	120	1.269	14.91	0.738	13.97	This work
2	FTO/c-TiO_2/$CsPbI_2Br$/carbon	340	1.15	13.54	0.642	10.0	3
3	ITO/SnO_2/Nb-$CsPbI_2Br$/carbon	160	1.20	12.06	0.72	10.42	4
4	FTO/Nb_2O_5/$Cs_{0.99}Rb_{0.01}PbI_2Br$/carbon	350	1.24	14.02	0.69	12	5
5	FTO/c-TiO_2/m-TiO_2/$CsPbI_2Br$/P3HT-MWCNT/carbon	280	1.21	13.35	0.62	10.01	6
6	ITO/SnO_2/$CsPbI_2Br$/PMMA/carbon	260	1.202	12.64	0.71	10.95	7
7	FTO/c-TiO_2/m TiO_2/Al_2O_3/NiO/carbon (embed $CsPbI_2Br$)	100	0.944	14.33	0.6250	8.44	7
8	ITO/SnO_2/$CsPbI_2Br$/carbon	180	1.187	12.91	0.661	10.13	9
9	FTO/c-TiO_2/$CsPbI_2Br$/carbon	280	1.15	13.87	0.64	10.21	10
10	ITO/SnO_2/$CsPbI_2Br$/carbon	150	1.14	14.25	0.6412	10.44	11
11	ITO/SnO_2/$CsPbI_2Br$/Co_3O_4/carbon	260	1.187	13.09	0.7212	11.21	12
12	ITO/SnO_2/$CsPbI_2Br$/SnPc/carbon	120	1.244	13.69	0.669	11.39	1
13	ITO/SnO_2/KOH/$CsPbI_2Br$/carbon	150	1.20	14.24	0.6871	11.78	13
14	FTO/c-TiO_2/m-TiO_2/$CsPbI_2Br$/carbon black/carbon	280	1.210	14.94	0.7259	13.13	14
15	ITO/c-TiO_2/m-TiO_2/Al_2O_3/NiO/carbon (embed $CsPb_{0.98}Mg_{0.02}I_2Br$)	280	1.063	14.75	0.69	10.8	15
16	ITO/SnO_2/$CsPbI_2Br$/CuPc derivative/carbon	120	1.223	13.61	0.663	11.04	2
17	FTO/TiO_2 NRAs/CsCl/$CsPbI_2Br$/carbon	260	1.15	14.39	0.691	11.45	16
18	FTO/c-TiO_2/m-TiO_2/$CsPb_{0.98}La_{0.02}I_2Br$/carbon	260	1.12	11.66	0.6124	8.03	17
19	FTO/SnO_2/$CsPbI_2Br$ (PbI_2-rich)/carbon	280	1.23	15.46	0.64	12.19	18
20	FTO/c-TiO_2/m-TiO_2/Al_2O_3/NiO/carbon (embed $CsPb_{0.5}Sn_{0.5}I_2Br$)	80	0.62	20.1	0.65	8.10	19
21	FTO/c-TiO_2/$CsPbI_2Br$/CuPc/PCCE	160	1.22	14.33	0.75	13.16	20
22	FTO/SnO_2/$CsPbI_2Br$ with PANI/carbon	280	1.33	14.29	0.7096	13.52	21
23	ITO/SnO_2/$CsPbI_2Br$/BrAL/carbon	260	1.205	13.68	0.688	11.34	22
24	FTO/c-TiO_2/$CsPbI_2Br$ (PbI_2-rich)/carbon	250	1.19	14.6	0.736	12.78	23
25	FTO/c-TiO_2/$BMIMPF_6$/$CsPbI_2Br$/carbon	250	1.22	14.33	0.7527	13.19	24
26	ITO/SnO_2/$CsPbI_2Br$/PEAI/carbon	280	1.3	14.508	0.7102	13.38	25
27	FTO/c-TiO_2/$CsPbI_2Br$/MABr/carbon	200	1.207	16.62	0.74	14.84	26

28	FTO/c-TiO_2/$CsPbI_2Br$/HTAB/carbon	270	1.26	14.1	0.806	14.3	27
29	FTO/c-TiO_2/m-TiO_2/$CsPbI_2Br$ with NaSCN/carbon	270	1.267	14.31	0.8066	14.63	28
30	FTO/c-TiO_2/$CsPbI_2Br$/carbon	160	1.17	14.84	0.7382	12.82	29
31	FTO/c-TiO_2/$CsPbI_2Br$/NPTMS/carbon	300	1.134	14.78	0.61	10.22	30
32	ITO/SnO_2/$SnCl_2$/$CsPbI_2Br$/Cs_2PtI_6/carbon	160	1.28	14.85	0.72	13.69	31
33	FTO/c-TiO_2/$TiCl_4$-$TiCl_3$/$CsPbI_2Br$/carbon	270	1.28	14.21	0.794	14.46	32
34	FTO/SnO_2/$SnCl_2$/$CsPbI_2Br$/carbon	160	1.22	14.83	0.72	13.01	33
35	FTO/c-TiO_2/$CsPbI_2Br$ with PVP/Spiro-OMeTAD/carbon	160	1.01	18.47	0.5635	10.47	34
36	FTO/SnO_2/$CsPbI_2Br$/TBAI/carbon	280	1.23	14.34	0.70	12.29	35
37	FTO/c-TiO_2/$CsPbI_2Br$ with $Mg(Ac)_2$/carbon	280	1.214	14.18	0.7590	13.08	36
38	FTO/SnO_2/$CsPbI_2Br$/delta-2:2-bis (1,3-dithiazole)/carbon	160	1.26	14.74	0.74	13.78	37
39	FTO/c-TiO_2/m-TiO_2/$CsPbI_2Br$/CNTs	250	1.12	14.17	0.712	11.31	38
40	ITO/SnO_2/$SnCl_2$/$CsPbI_2Br$/$BMIMBF_4$/carbon	160	1.27	14.68	0.75	14.03	39
41	ITO/SnO_2/$CsPbI_2Br$ with MAAc/carbon	280	1.27	14.2	0.618	11.2	40
42	FTO/Nb_2O_5/$Cs_{0.99}Rb_{0.01}PbI_2Br$/carbon	150	1.23	13.8	0.66	11.2	5
43	FTO/c-TiO_2/$CsPbI_2Br$/carbon	250	1.164	16.09	0.71	13.30	41
44	ITO/c-TiO_2/$CsPbI_2Br$/ATHPBr/carbon	160	1.30	14.28	0.7811	14.50	42
45	FTO/c-TiO_2/m-TiO_2/$CsPbI_2Br$ with MPA-CdSe QDs/carbon	270	1.25	14.47	0.801	14.49	43
46	FTO/c-TiO_2/$CsPbI_2Br$/MoO_2&PTAA/carbon	150	1.18	13.93	0.7852	12.91	44
47	FTO/SnO_2/$CsPbI_2Br$ with PA/carbon	130	1.28	13.64	0.625	10.95	45
48	FTO/c-TiO_2/m-TiO_2/$CsPbI_2Br$/Cs_2SnI_6/carbon	270	1.267	14.51	0.7981	14.67	46
49	FTO/c-TiO_2/$CsPbI_2Br$/carbon	300	1.09	16.59	0.7240	13.07	47
50	FTO/c-TiO_2/$CsPbI_2Br$/carbon	250	1.312	15.70	0.74	15.24	48

Table S8. Photovoltaic parameters of carbon-based $CsPbI_2Br$ PSCs measured under the *RS* and *FS* directions.

Device	Scan direction	V_{oc} (V)	J_{sc} (mA cm^{-2})	FF	PCE (%)	HI
Reference	*RS*	1.217	14.69	0.681	12.18	0.102
	FS	1.208	14.46	0.626	10.94	
PEAI	*RS*	1.244	14.81	0.720	13.27	0.036
	FS	1.222	14.60	0.717	12.79	
PEABr	*RS*	1.254	14.84	0.726	13.51	0.022
	FS	1.247	14.68	0.722	13.22	
P-F-PEAI	*RS*	1.261	14.88	0.740	13.89	0.035
	FS	1.253	14.72	0.727	13.41	
P-F-PEABr	*RS*	1.269	14.91	0.738	13.97	0.019
	FS	1.265	14.79	0.732	13.70	

Table S9. Detailed parameters derived from the UPS spectra for reference and passivated $CsPbI_2Br$ films.

Sample	E_{offset}	E_{onset}	E_g	W_F	VBM	CBM
Reference	16.87	1.71	1.88	-4.35	-6.06	-4.18
PEAI	17.07	1.83	1.87	-4.15	-5.98	-4.11
PEABr	17.13	1.85	1.89	-4.09	-5.94	-4.05
P-F-PEAI	17.20	1.86	1.87	-4.02	-5.88	-4.01
P-F-PEABr	17.26	1.87	1.89	-3.96	-5.83	-3.94

Table S10. Fitting parameters of TPV of reference and passivated devices.

Device	A_3	τ_3 (ms)	τ_3 (%)	A_4	τ_4 (ms)	τ_4 (%)	τ_{TPV} (ms)
Reference	0.87	1.12	0.12	0.32	22.98	0.88	20.42
PEAI	1.17	0.89	0.13	0.37	18.45	0.87	16.13
PEABr	1.76	0.54	0.18	0.24	17.91	0.82	14.77
P-F-PEAI	0.64	1.58	0.16	0.45	12.17	0.84	10.52
P-F-PEABr	0.24	0.90	0.03	0.75	10.51	0.97	10.25

Table S11. Fitting values of different parameters obtained from the Nyquist plots of reference and passivated devices measured at a bias of 1.20 V under light illumination.

Device	R_s (Ω·cm^2)	R_{tra} (Ω·cm^2)	R_{rec} (Ω·cm^2)	CPE_{tra}-T (nF cm^{-2})	CPE_{tra}-P	CPE_{rec}-T (×10^6 nF cm^{-2})	CPE_{rec}-P
Reference	2.59	163.4	583.38	215.9	0.950	1.31	0.552
PEAI	2.17	144.0	605.20	110.4	0.998	1.76	0.607
PEABr	2.14	126.7	700.56	211.3	0.937	2.31	0.480
P-F-PEAI	1.55	111.0	1069.11	312.0	0.926	2.60	0.460
P-F-PEABr	1.04	92.3	1089.00	104.4	0.999	3.05	0.517

Table S12. The n and α values of reference and passivated devices extracted from **Figure 5f** and **S14**.

Device	Reference	PEAI	PEABr	P-F-PEAI	P-F-PEABr
n	1.89	1.71	1.69	1.67	1.63
α	0.975	0.981	0.983	0.984	0.986

References

1 X. Zhang, N. Gao, Y. Li, L. Xie, X. Yu, X. Lu, X. Gao, J. Gao, L. Shui, S. Wu and J.-M. Liu, *ACS Appl. Energy Mater.*, 2020, **3**, 7832-7843.

2 X. Zhang, J. Yang, L. Xie, X. Lu, X. Gao, J. Gao, L. Shui, S. Wu and J.-M. Liu, *Dye. Pigm.*, 2021, **186**, 109024.

3 C. Dong, X. Han, Y. Zhao, J. Li, L. Chang and W. Zhao, *Sol. RRL*, 2018, **2**, 1800139.

4 Z. Guo, S. Zhao, A. Liu, Y. Kamata, S. Teo, S. Yang, Z. Xu, S. Hayase and T. Ma, *ACS Appl. Mater. Interfaces*, 2019, **11**, 19994-20003.

5 Y. Guo, F. Zhao, J. Tao, J. Jiang, J. Zhang, J. Yang, Z. Hu and J. Chu, *ChemSusChem*, 2019, **12**, 983-989.

6 G. Wang, J. Liu, K. Chen, R. Pathak, A. Gurung and Q. Qiao, *J. Colloid Interf. Sci.*, 2019, **555**, 180-186.

7 X. Zhang, Y. Zhou, Y. Li, J. Sun, X. Lu, X. Gao, J. Gao, L. Shui, S. Wu and J.-M. Liu, *J. Mater. Chem. C*, 2019, **7**, 3852-3861.

8 T. Zhang, H. Li, S. Liu, X. Wang, X. Gong, Q. Sun, Y. Shen and M. Wang, *J Phys. Chem. Lett.*, 2019, **10**, 200-205.

9 X. Meng, Z. Wang, W. Qian, Z. Zhu, T. Zhang, Y. Bai, C. Hu, S. Xiao, Y. Yang and S. Yang, *J. Phys. Chem. Lett.*, 2019, **10**, 194-199.

10 C. Dong, X. Han, W. Li, Q. Qiu and J. Wang, *Nano Energy*, 2019, **59**, 553-559.

11 Z. Ye, J. Zhou, J. Hou, F. Deng, Y.-Z. Zheng and X. Tao, *Sol. RRL*, 2019, **3**, 1900109.

12 Y. Zhou, X. Zhang, X. Lu, X. Gao, J. Gao, L. Shui, S. Wu and J.-M. Liu, *Sol. RRL*, 2019, **3**, 1800315.

13 F. Deng, X. Li, X. Lv, J. Zhou, Y. Chen, X. Sun, Y.-Z. Zheng, X. Tao and J.-F. Chen, *ACS Appl. Energy Mater.*, 2020, **3**, 401-410.

14 S. Gong, H. Li, Z. Chen, C. Shou, M. Huang and S. Yang, *ACS Appl. Mater. Interfaces*, 2020, **12**, 34882-34889.

15 S. Liu, L. Guan, T. Zhang, X. Gong, X. Zhao, Q. Sun, X. Shai, X. L. Zhang, X. Xiao, Y. Shen and M. Wang, *Appl. Mater. Today*, 2020, **20**, 100644.

16 W. Cai, Y. Lv, K. Chen, Z. Zhang, Y. Jin and X. Zhou, *Energy Fuels*, 2020, **34**, 11670-11678.

17 S. Chen, T. Zhang, X. Liu, J. Qiao, L. Peng, J. Wang, Y. Liu, T. Yang and J. Lin, *J. Mater. Chem. C*, 2020, **8**, 3351-3358.

18 C. Liu, M. Wu, Y. Wu, D. Wang and T. Zhang, *J. Power Sources*, 2020, **447**, 227389.

19 H. Ban, Q. Sun, T. Zhang, H. Li, Y. Shen and M. Wang, *Sol. RRL*, 2020, **4**, 1900457.

20 P. Xie, G. Zhang, Z. Yang, Z. Pan, Y. Fang, H. Rao and X. Zhong, *Sol. RRL*, 2020,

4, 2000431.

21 C. Liu, J. He, M. Wu, Y. Wu, P. Du, L. Fan, Q. Zhang, D. Wang and T. Zhang, *Sol. RRL*, 2020, **4**, 2000016.

22 Y. Li, J. Yang, L. Xie, Y. Li, X. Liang, X. Lu, X. Gao, J. Gao, L. Shui, S. Wu and J.-M. Liu, *ACS Appl. Energy Mater.*, 2021, **4**, 5415-5423.

23 K. Wang, T. You, R. Yin, B. Fan, J. Liu, S. Cui, H. Chen and P. Yin, *ACS Appl. Energy Mater.*, 2021, **4**, 3508-3517.

24 R. Yin, K.-X. Wang, S. Cui, B.-B. Fan, J.-W. Liu, Y.-K. Gao, T.-T. You and P.-G. Yin, *ACS Appl. Energy Mater.*, 2021, **4**, 9294-9303.

25 Y. Wu, Q. Zhang, L. Fan, C. Liu, M. Wu, D. Wang and T. Zhang, *ACS Appl. Energy Mater.*, 2021, **4**, 5583-5589.

26 W. Zhu, W. Chai, D. Chen, J. Ma, D. Chen, H. Xi, J. Zhang, C. Zhang and Y. Hao, *ACS Energy Lett.*, 2021, **6**, 1500-1510.

27 G. Zhang, P. Xie, Z. Huang, Z. Yang, Z. Pan, Y. Fang, H. Rao and X. Zhong, *Adv. Funct. Mater.*, 2021, **31**, 2011187.

28 Z. Yang, G. Zhang, J. Zhang, Z. Pan, S. Yang, B. Liu, H. Rao and X. Zhong, *Chem. Eng. J.*, 2022, **430**, 133083.

29 W. Su, X. Han, J. Feng, Z. Zhu, H. Huang, J. Li, T. Yu, Z. Li and Z. Zou, *Energy Fuels*, 2021, **35**, 11488-11495.

30 J. Yu, W. Li, K. Zhang and X. Han, *J. Mater. Sci.: Mater. Electron.*, 2021, **32**, 20936-20945.

31 Q. Han, S. Yang, L. Wang, F. Yu, X. Cai and T. Ma, *J. Colloid Interf. Sci.*, 2022, **606**, 800-807.

32 W. Wang, Y. Lin, G. Zhang, C. Kang, Z. Pan, X. Zhong and H. Rao, *J. Energy Chem.*, 2021, **63**, 442-451.

33 Q. Han, F. Yu, L. Wang, S. Yang, X. Cai, X. Meng, O. Yūta, K. Takeshi, C. Zhang and T. Ma, *J. Power Sources*, 2021, **516**, 230676.

34 S. Ullah, P. Yang, J. Wang, L. Liu, S.-E. Yang, T. Xia and Y. Chen, *J. Solid State Chem.*, 2022, **305**, 122656.

35 S. Zheng, H. Wang, P. Wei, H. Chen and Y. Xie, *Sol. Energy*, 2021, **230**, 666-674.

36 K. Zhang, W. Li, J. Yu and X. Han, *Sol. Energy*, 2021, **222**, 186-192.

37 Q. Han, S. Yang, L. Wang, F. Yu, C. Zhang, M. Wu and T. Ma, *Sol. Energy*, 2021, **216**, 351-357.

38 Z. Dong, W. Li, H. Wang, X. Jiang, H. Liu, L. Zhu and H. Chen, *Sol. RRL*, 2021, **5**, 2100370.

39 F. Yu, Q. Han, L. Wang, S. Yang, X. Cai, C. Zhang and T. Ma, *Sol. RRL*, 2021, **5**, 2100404.

40 X. Li, Y. Zhang, G. Liu, Z. Zhang, L. Xiao, Z. Chen and B. Qu, *ACS Appl. Energy Mater.*, 2021, **4**, 13444-13449.

41 Z. Zhang, Y. Ba, D. Chen, J. Ma, W. Zhu, H. Xi, D. Chen, J. Zhang, C. Zhang and Y. Hao, *iScience*, 2021, **24**, 103365.

42 Z. Yan, D. Wang, Y. Jing, X. Wang, H. Zhang, X. Liu, S. Wang, C. Wang, W. Sun, J. Wu and Z. Lan, *Chem. Eng. J.*, 2022, **433**, 134611.

43 S. Xu, C. Kang, Z. Huang, Z. Zhang, H. Rao, Z. Pan and X. Zhong, *Sol. RRL*, 2022, **6**, 2100989.

44. D. S. Lee, M. J. Ki, H. J. Lee, J. K. Park, S. Y. Hong, B. W. Kim, J. H. Heo and S. H. Im, *ACS Appl. Mater. Interfaces*, 2022, **14**, 7926-7935.

45 X. Xu, W. Qin, S. Liu, C. Xing, G. Ge, D. Wang and T. Zhang, *Org. Electron.*, 2022, **103**, 106463.

46 G. Zhang, J. Zhang, Y. Liao, Z. Pan, H. Rao and X. Zhong, *Chem. Eng. J.*, 2022, **440**, 135710.

47 J. Lv, W. Zhao, W. Li, J. Yu, M. Zhang, X. Han and T. Tanaka, *J. Mater. Chem. C*, 2022, **10**, 4276-4285.

48 W. Zhu, J. Ma, W. Chai, T. Han, D. Chen, X. Xie, G. Liu, P. Dong, H. Xi, D. Chen, J. Zhang, C. Zhang and Y. Hao, *Sol. RRL*, 2022, **6**, 2200020.